RESEARCH/REVIEW ARTICLE

Coastal erosion dynamics on the permafrost-dominated Bykovsky Peninsula, north Siberia, 1951–2006

Hugues Lantuit,[1] David Atkinson,[2] Pier Paul Overduin,[1] Mikhail Grigoriev,[3] Volker Rachold,[4] Guido Grosse[5] & Hans-Wolfgang Hubberten[1]

[1] Alfred Wegener Institute for Polar and Marine Research, Telegrafenberg A43, DE-14473 Potsdam, Germany
[2] International Arctic Research Centre, University of Alaska Fairbanks, P.O. Box 757340, Fairbanks, AK 99775-7340, USA
[3] Permafrost Institute of the Siberian Division of the Russian Academy of Science, RU-677010 Yakutsk, Russia
[4] International Arctic Science Committee, Telegrafenberg A43, DE-14473 Potsdam, Germany
[5] Geophysical Institute, University of Alaska Fairbanks, 903 Koyukuk Drive, Fairbanks, AK 99775-7320, USA

Keywords
Coastal erosion; permafrost; Arctic; climate change; Russia.

Correspondence
Hugues Lantuit, Alfred Wegener Institute for Polar and Marine Research, Telegrafenberg A43, DE-14473 Potsdam, Germany.
E-mail: hugues.lantuit@awi.de

Abstract

This study investigates the rate of erosion during the 1951–2006 period on the Bykovsky Peninsula, located north-east of the harbour town of Tiksi, north Siberia. Its coastline, which is characterized by the presence of ice-rich sediment (Ice Complex) and the vicinity of the Lena River Delta, retreated at a mean rate of 0.59 m/yr between 1951 and 2006. Total erosion ranged from 434 m of erosion to 92 m of accretion during these 56 years and exhibited large variability ($\sigma = 45.4$). Ninety-seven percent of the rates observed were less than 2 m/yr and 81.6% were less than 1 m/yr. No significant trend in erosion could be recorded despite the study of five temporal subperiods within 1951–2006. Erosion modes and rates actually appear to be strongly dependant on the nature of the backshore material, erosion being stronger along low-lying coastal stretches affected by past or current thermokarst activity. The juxtaposition of wind records monitored at the town of Tiksi and erosion records yielded no significant relationship despite strong record amplitude for both data sets. We explain this poor relationship by the only rough incorporation of sea-ice cover in our storm extraction algorithm, the use of land-based wind records vs. offshore winds, the proximity of the peninsula to the Lena River Delta freshwater and sediment plume and the local topographical constraints on wave development.

Coastal erosion in the Arctic differs from its counterpart in temperate regions due to the short open-water season (3–4 months) and to the presence of ice in the marine and terrestrial environments (that is, permafrost and ground ice). Despite these restrictions, Arctic coastal erosion rates compare with temperate coastal erosion and lead to the release of vast quantities of terrestrial organic carbon and contaminants to the Arctic Ocean (Rachold et al. 2000; Rachold et al. 2003).

Storms, which are the largest driver of erosion (Solomon & Covill 1995), occur throughout the year but their impact is limited due to the presence of sea-ice cover during the fall, winter and spring (Atkinson 2005). Even during the summer period, chunks of sea ice in various quantities can impede the development of waves in the shore zone. Coastal retreat rates are also highly variable both spatially and temporally (Rachold et al. 2000; Solomon 2005; Lantuit & Pollard 2008). Spatial variability is mainly due to variations in the lithology, cryology and geomorphology of coastal cliffs. Temporal variability is related to the variation of the climatic forcing, which affects the degree of storminess, thermal conditions and sea-ice conditions in the coastal zone (Solomon et al. 1994).

An unique feature of Arctic polar coastal systems is ground ice: all types of ice contained in freezing and frozen ground, with a distinction between pore ice and segregated ice (van Everdingen 1998). It is present in the

Citation: *Polar Research* 2011, *30*, 7341, DOI: 10.3402/polar.v30i0.7341

subaerial part of the shore profile (see Fig. 1, for example) but also underneath the water column as submarine ground ice (Mackay 1972; Rachold et al. 2007). Its presence affects both the response of the shore to thermal–hydrodynamical forcing and the sediment budget of the coast (Aré 1988; Dallimore et al. 1996). The presence of ground ice leads to thermal abrasion (Aré 1988), a process that encompasses the combined kinetic action of waves and thawing of ground ice. Upon melting it enhances coastal zone susceptibility to erosion (Héquette & Barnes 1990; Kobayashi et al. 1999), especially when present as massive ice in coastal cliffs or through the occurrence of large thermokarst features in the coastal zone (Wolfe et al. 2001; Jorgenson & Brown 2005; Lantuit & Pollard 2005; Jones et al. 2008; Lantuit & Pollard 2008).

The very high rates of erosion observed on many Arctic coasts, exceeding that observed on many temperate coasts exposed to year-round wave activity (Rachold et al. 2000), suggests contribution from mechanisms in addition to thaw and kinetic erosion. Dallimore et al. (1996) suggested that thaw settlement of ice-rich sediments in the nearshore zone could induce a change in the shoreface profile and so support larger and more powerful waves. However, not all Arctic coastlines are characterized by subsea ice-rich permafrost and other explanations must be sought. Héquette & Barnes (1990) studied statistically the relationship between erosion rates and hydrodynamic and geomorphic factors and concluded on the necessary involvement of an additional force to drive the strong retreat rates. They attributed those to the occurrence of ice scours and sediment entrainment by sea ice in the offshore zone. As shown by Forbes & Taylor (1994), these can alter significantly the coastal sediment budget.

The Bykovsky Peninsula is located north-east of the harbour town of Tiksi in the northernmost part of Siberia (Fig. 2) and forms a natural protection for the harbour. Tiksi was founded in the 1930s and rapidly grew as a hub for shipping on the Northern Sea Route, which links the Bering Strait to northern Europe through Russian Arctic waters. The collapse of the Soviet Union led to the virtual abandonment of the industrial harbour but projections of reduced sea-ice cover during the summer months have provided an incentive to operate the Northern Sea Route again. Tiksi, which is sheltered from storms by the Bykovsky Peninsula, is of crucial importance as part of these plans (Matushenko 2000). The peninsula is characterized by the presence of ice-rich sediment (Ice Complex) and exhibits large rates of erosion induced by periodic storms and thermal–mechanical erosion of ice-rich sediments. These rates have been estimated at 2–6 m/yr, with highs of 20 m/yr (Aré 1988; Rachold et al. 2000). These rate estimates were extrapolated measurements from a few survey sites, however, and have not considered the spatial and temporal variability of coastal erosion on the peninsula. The potential increased exploitation of the Northern Sea Route, encouraged by the continued retreat of the polar ice pack and the subsequent expected increasing activity in Tiksi Bay (Matushenko 2000), provide an incentive to undertake in this region a more spatially detailed examination of erosion rates and to consider in greater depth possible driving mechanisms. The modification of the Bykovsky Peninsula shoreline could directly impact the harbour infrastructure. In light of this, this paper has two objectives: (1) to build a spatially comprehensive and updated compilation of coastal retreat rates from the Bykovsky Peninsula based on aerial photography (1951, 1981, 1986) and satellite imagery (1964, 1969, 1975, 2006); and (2) to analyse these data

Fig. 1 Ice Complex deposits (ground ice) exposed at the coast of the Bykovsky Peninsula. Note the thermo-erosional notch at the land–water interface, highlighted by white arrows.

Citation: *Polar Research* 2011, *30*, 7341, DOI: 10.3402/polar.v30i0.7341

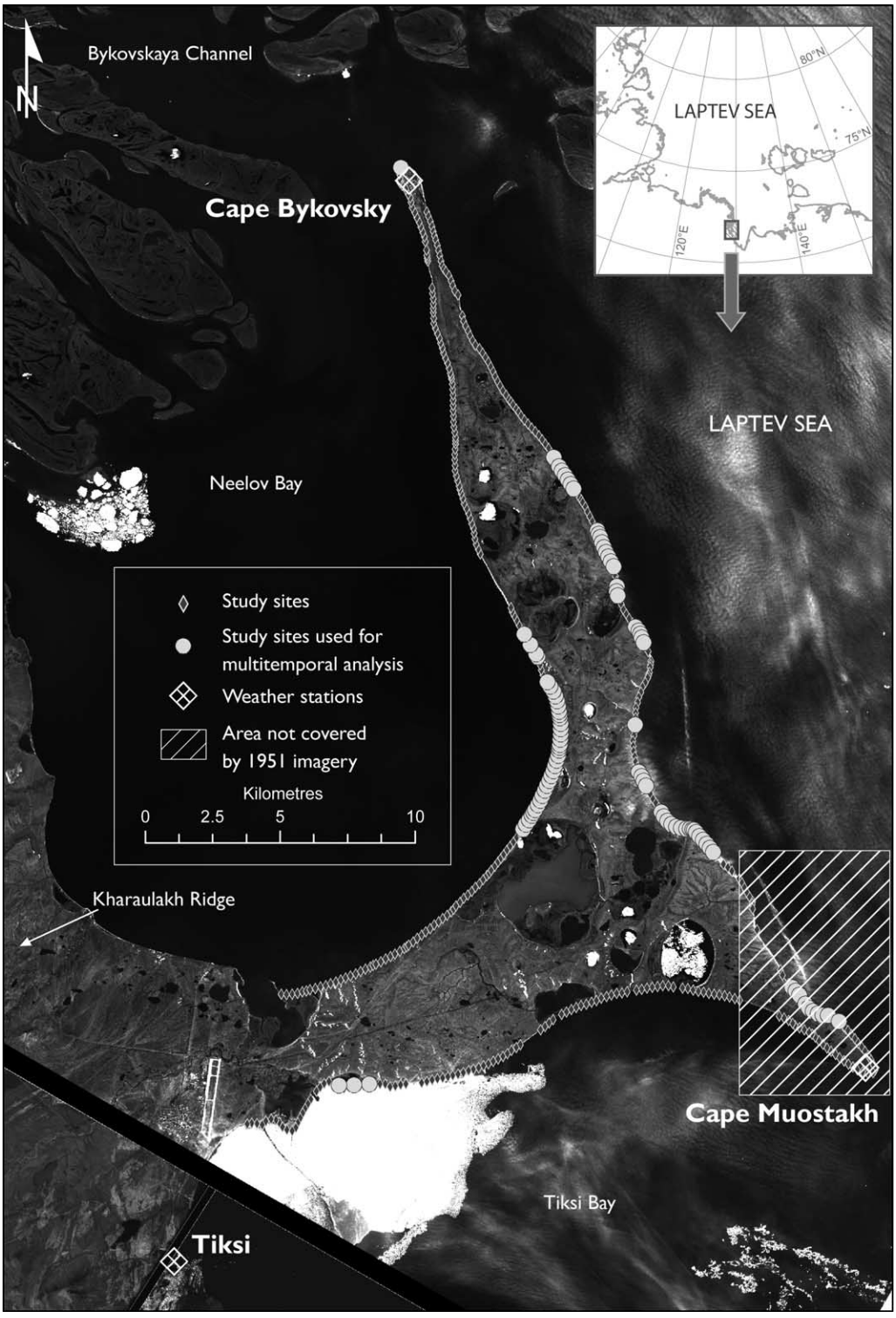

Fig. 2 Study area: the Bykovsky Peninsula is located near to the mouth of the Lena River and forms a natural protection for the harbour of Tiksi (1969 Corona KH-4 imagery).

with respect to new information about coastal environmental forcing, including seasonal wind/storm activity.

The resulting data set and analysis results, in combination with forecast/hindcast scenarios of environmental forcing, can be used to predict future rates of erosion using shoreline modelling techniques such as the end-point rate method (Dolan et al. 1991), refine regional sediment budgets, assess the temporal variability of erosion over the second half of the 20th century and, ultimately, aid planning and infrastructure development.

Study area

Location

The Bykovsky Peninsula extends in a NNW–SSE orientation at the tip of one of the outflow channels of the Lena River Delta (Bykovskaya Channel), at the foot of the Kharaulakh Ridge. It lies within the zone of continuous permafrost that reaches depths of 500–600 m in the region (Grigor'ev et al. 1996). The peninsula is located in the Polar Tundra zone of the Köppen–Geiger world climate classification (Peel et al. 2007) and, although located on a coast, experiences large seasonal temperature variations suggesting an almost continental climate (–12°C mean annual temperature). The open-water season in the southern Laptev Sea extends on average from mid-June to mid-October but can begin as early as late May. In 1993, open water was present off the landfast ice zone by May 26. The ice-free period has extended as late as the third week in October (1985). However, in most cases, fast ice persists until mid-June and it is not rare to see blocks of pack ice in July along the coast.

Physiography

The Bykovsky Peninsula is underlain by extensive Ice Complex deposits (Schirrmeister et al. 2002) and reaches up to 45 m a.s.l. The Ice Complex is "an ice-rich unconsolidated permafrost deposit with a large content of ice wedges" (Aré 1988: 11). The ice wedges on the Bykovsky Peninsula are up to 5 m in width and up to 40–50 m in depth (Meyer et al. 2002); single ice wedges coalesce and together with the sediments in between and the segregated ground ice it forms the Ice Complex. The Ice Complex deposits are made of poorly sorted sandy silt to silty sand with frequent presence of peat layers and palaeosoils and are remarkably homogeneous from a sedimentological standpoint (Siegert et al. 2002). Holocene deposits, usually lacustrine silt and peat-rich soils, are found as a cover layer on top of the Ice Complex and in basins and valleys formed by thermokarst. They largely consist of reworked sediments of the Ice Complex, often with enrichment of organic matter in thick peat horizons.

The two dominant backshore coastal landforms in the study area are cliffs and low-lying topographical depressions. Cliff morphology ranges from relatively stable, vegetated slopes to nearly vertical cliffs, reaching 45 m in some places and often containing exposures of Ice Complex sediments and ice wedges. Subaerial cliff erosion (thermal denudation) is dominated by the occurrence of large retrogressive thaw slumps, often extending along as much as a kilometre of shoreline and up to several hundred metres inland.

The low-lying depressions are thermokarst basins formed by thawing of ice-rich permafrost and subsequent surface subsidence. About 46% of the Bykovsky Peninsula is covered by such basins (Grosse et al. 2005). In some basins, middle Holocene lake drainage by tapping from coastal erosion has resulted in the subsequent formation of thick peat horizons and the establishment of various periglacial features, including refreezing of the lacustrine sediments, re-accumulation of ground ice and the growth of ice wedges up to 2 m in width (Grosse et al. 2007). Six pingos (formed by refreezing of thawed drained lake sediments) with heights up to 28 m a.s.l. are located in thermokarst basins on the peninsula.

The Ice Complex once covered vast areas on the Laptev Sea Shelf (Romanovskii et al. 2000), which was progressively flooded during the postglacial sea-level rise. Sea level reached its current elevation at around 5000 BP (Bauch et al. 2001), giving the Bykovsky Peninsula approximately its current shape.

The position of the peninsula in the axis of the Bykovskaya Channel, which is one of the largest of the Lena River outflow channels by discharge (Pavlova & Dorozhkina 2002), induces the presence of brackish water along east coasts throughout the spring melt discharge period. The peninsula is surrounded by relatively shallow waters (Fig. 3) with depths exceeding 10 m only on the southern shore facing the Tiksi Bay, directly at the outlet of the Bykovskaya Channel. About 25% of the Lena's spring discharge exits the delta through the south-eastern Bykovskaya Channel. In the absence of field measurements of seasonal sea bottom water temperatures, which are difficult to obtain due to sea-ice dynamics, it is usually assumed that the bottom water temperature on the shelf is relatively stable at around −1.8°C (Romanovskii & Hubberten 2001). At the outlet of the Bykovskaya Channel, mean sea bottom water temperature recorded using a conductivity/temperature data logger for the one-year period from September

Citation: *Polar Research* 2011, *30*, 7341, DOI: 10.3402/polar.v30i0.7341

2007–August 2008 at a water depth of 7 m, 4.5 km from shore, was 2.3°C. Seasonally, temperature lay between −1.4 and 0.0°C for more than eight months of the year, but summer temperatures reach almost 16.0°C (Fig. 4). In July and August water temperatures remained above 6.0°C. The measured temperatures remain below those measured at the Stolb hydrological station in the Lena Delta (Yang et al. 2005), but follow the temporal trend of mean river water temperature during the ice-free period. Mean conductivity (an indication of salinity) for the three data loggers lay at 12.2 mS cm^{-1}. Summer salinity was low, reflecting the fluvial source of water along the coast. For the eight months of low temperature water, the electrical conductivity exceeded 10.0 mS cm^{-1}.

Sea level

The tidal regime in Bykovsky Peninsula is micro-tidal and tidally-based sea-level oscillations have little influence on the height of storm surges. The influence of the Lena River is, however, substantial. At Bykovsky Mys, a settlement at the north end of the Bykovsky Peninsula, sea-level recording data are available continuously from summer 1976 until the end of 1987, and intermittently since then. Sea-level data for the Arctic are based on these data and other data sets available from the Woods Hole Oceanographic Institution, funded by the US National Oceanic and Atmospheric Administration and the US National Science Foundation (http://www.whoi.edu/science/PO/arcticsealevel/index.html). These data, which are described on the website and in numerous publications online (e.g., Fetterer 2008), indicate that sea level at the north end of the Bykovsky Peninsula is strongly controlled by the spring river discharge melt event, and varies up to 1.1 m annually. The annual minimum monthly mean occurs between August and December, and is probably controlled by a number of factors. The high stand occurs in June of each year, and is the result of ice out and the spring snowmelt discharge event. This abrupt increase in sea level is also incidentally occurring when sea ice is largely present around the shores of the peninsula, which limits the impact of high-water stands on the intensity of erosion. Continuous records are also available from Tiksi (since 1949) and Muostakh Island (1951–1995), south of the Bykovsky Peninsula, and show a slightly lower annual amplitude (up to 0.9 m) in mean monthly sea level. Both continuous data sets record an increasing trend in sea level over the period of record of this study.

Table 1 Imagery used in the study. All scenes have been resampled to a 2.5 m spatial resolution.

Date	Type	Original ground resolution	Image identification no.	Root mean square (m)
08-04-1951	Greyscale aerial photography	1:68 000 (2.5 m)	II-51-11118	7.81
08-04-1951				
08-04-1951				
08-04-1951				
08-04-1951				
08-04-1951				
08-25-1951				
	Greyscale aerial photography		II-51-11162	7.97
	Greyscale aerial photography		II-51-11167	9.99
	Greyscale aerial photography		II-51-11217	9.51
	Greyscale aerial photography		II-51-11219	4.58
	Greyscale aerial photography		II-51-11221	3.64
	Greyscale aerial photography		II-51-12276	4.90
06-22-1964	Corona KH-4B	2.5 m	D003003m1107-1AFT	10.11
	Corona KH-4B		D003002m1107-1AFT	8.13
07-24-1969	Corona KH-4	2.5 m	036019dsfwd1007-1	9.63
	Corona KH-4		036020dsfwd1007-1	11.71
07-17-1975	Hexagon KH-9	2.5 m	R06221550101210-5	0.00
08-08-1981	Greyscale aerial photography	1:47 400 (2 m)	3-914-81-94	5.74
	Greyscale aerial photography		3-914-81-96	3.76
	Greyscale aerial photography		3-914-81-98	4.64
	Greyscale aerial photography		3-914-81-105	5.24
	Greyscale aerial photography		3-914-81-125	8.84
	Greyscale aerial photography		3-914-81-128	7.32
1986	Resurs KFK 1000	5 m	Resurs KFK 1000	12.02
07-09-2006	SPOT-5 (panchromatic)[a]	2.5 m	5 085-017/5 06/07/09 03:41:47 1 T	8.64

[a]Satellite Pour l'Observation de la Terre.

Table 2 Imagery georeferencing and dilution of accuracy (DOA) for the 96 subsampled points used in the temporal analysis. The periods for which the margin of error is greater than 25% of the measured average rate are in boldface.

Date	Maximum DOA (m)	Average retreat (m)
1951–1964	1.11	20.22
1964–69	**3.13**	**5.89**
1969–1975	2.00	9.73
1975–1981	1.53	12.36
1981–86	**3.03**	**7.83**
1986–2006	0.75	21.83
1981–2006	0.50	38.85

On average, maximum wave heights are between 1.0 and 1.1 m during storms in the Tiksi Bay and between 0.6 and 0.8 m in the Neelov Bay based on records dating back to the 1980s (Sukhovey 1986). The same records indicate a maximum recorded storm surge of 1.5 m in Tiksi Bay and less than a metre in the Neelov Bay, which seems to indicate a potential substantial influence of onshore winds on the erosional process in the latter location.

Coastal erosion

The erosion of Bykovsky Peninsula coasts has been the subject of detailed investigations since Adams launched scientific investigations in the region and discovered the first entire mammoth on the peninsula in 1799 (Adams 1807). Subsequent investigators provided considerable information on the geomorphology of its coasts, including coastal erosion rates (Hmiznikov 1937; Kljuev 1970). In the 1980s, Aré (1988) compiled a detailed summary focussing on processes acting upon Arctic coasts with large passages dedicated to the Bykovsky Peninsula. Grigor'ev et al. (1996) and Rachold et al. (2000) provided the most recent update of coastal erosion rates for the period 1951–1999 based on airphoto imagery and ground-based measurements but focused on short stretches of coast along the peninsula. They published two retreat rates (2.0 and 2.7 m/yr for two sections on the north-east coast of the peninsula. Aré (1988) highlighted the high spatial and temporal variability of coastal erosion on the peninsula, a phenomenon observed also elsewhere in the Arctic (Solomon 2005; Lantuit & Pollard 2008). In particular, he noted the apparently random occurrence of periods of intense erosion followed by periods of stabilization of the coast. He related those to several factors, including the occurrence of subaerial thermal denudation features, differences in coastal lithology and/or morphology and a possible cyclical evolution of the shoreface profile. The tidal regime in the Bykovsky Peninsula is micro-tidal and tidally based sea-level oscillations have little influence on the height of storm surges. The intensity of erosion is therefore thought to be largely correlated only to the strength of storm-wind driven waves and water-level surges.

Establishing clear direction in this question, however, is hampered by lack of a continuous record of erosion for Bykovsky Peninsula. This limits the explanatory power of results derived from statistical relations of erosion to meteorological factors.

Storm climatology

Storm activity in the vicinity of the Lena River Delta and the broader region of the Laptev Sea consists mostly of transient systems migrating into the region from two main directions: over the continent from the south-west and along the northern coast from the west (Arctic Climatology Project 2000). Little local storm formation is observed. Storm activity, defined in this case as storm counts, varies over the course of a year with a peak in activity coming in late summer/early fall, coincident with maximum ice-free period (Atkinson 2005). This is in contrast with north Russian coastal zones to the east and west, which are both more strongly dominated by the proximity of Atlantic/Pacific sector storm activity and that shows up as a frequency peak occurring later in the year in October/November. Storms in this area tend to be, on average, 43 hours in duration and reach wind speeds of 10.3 m/s. There has been no particular trend in coastal storm activity in this region observed since 1950, although there was a marked jump from one activity level to another that occurred in the mid-1970s. This was consistent with other north Russian coastal regions as well as indicators of atmospheric circulation changes that occurred at this time (Savelieva et al. 2000; Semiletov et al. 2000).

Methods

Geoprocessing of airborne and spaceborne imagery

We used aerial photographs and remote-sensing imagery from a variety of sensors (Corona, Hexagon, Resurs-R KFA 1000 and Satellite Pour l'Observation de la Terre [SPOT]-5) to both extend the time range of the study and to obtain better temporal resolution (Table 1). Geoprocessing of aerial photographs and satellite imagery was conducted to obtain a ± 2.5 m horizontal accuracy for images of the Bykovsky Peninsula coastline from 1951, 1964, 1969, 1975, 1981, 1986 and 2006. The aerial photographs as well as the Resurs-R KFA 1000 image

Citation: *Polar Research* 2011, *30*, 7341, DOI: 10.3402/polar.v30i0.7341

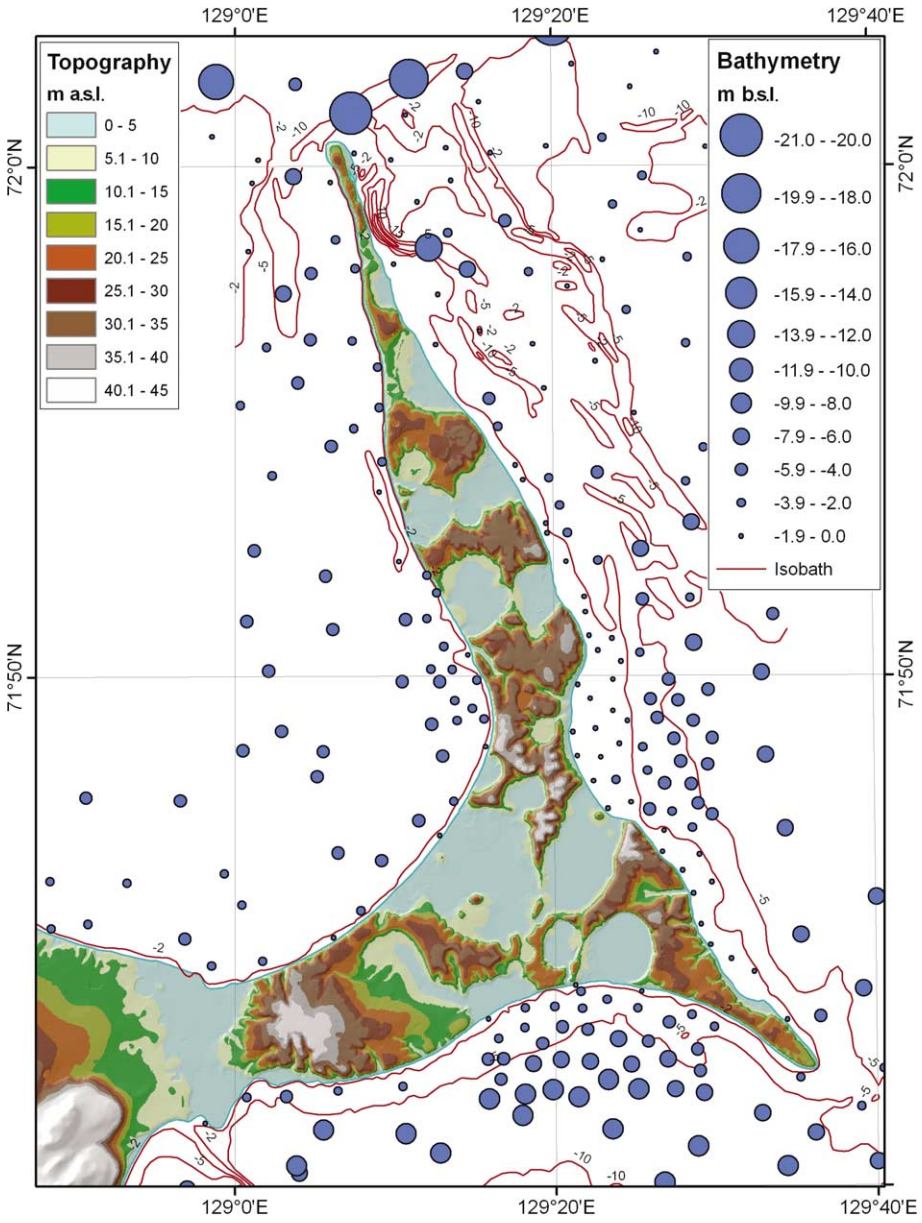

Fig. 3 Subaqueous setting of the study area. The Bykovsky Peninsula is surrounded by fairly shallow waters with depths exceeding 10 m only in the Tiksi Bay and at the outlet of the Bykovskaya Channel.

were obtained from the Russian national archives, while the declassified Corona and Hexagon imagery and the SPOT-5 imagery were purchased through commercial portals. All images were resampled to a standard 2.5 m nadir resolution. The Hexagon and Resurs KFA-1000 1986 images were originally acquired at lower resolution and their original resolution is about 7–8 m. The limited quality of the KFA-1000 image, which was available only as hardcopy paper print, reduced its value for the interpretation of coastal retreat.

The lack of a reliable net of ground control points in the area as well as the difficulties in getting authorization to use a high-precision differential global positioning system induced some constraints for the georeferencing process. Unlike similar studies (Lantuit & Pollard 2008), which were able to utilize absolute georeferencing based on a fixed number of surveyed ground control points, the present study used image co-referencing to the best available data source. In other words, the images were not georeferenced to absolute ground control points.

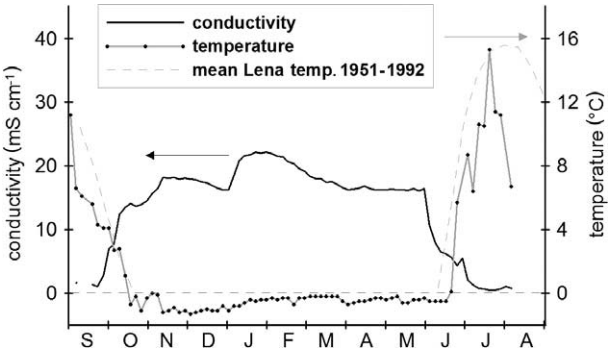

Fig. 4 Sea bottom water temperature and conductivity (which corresponds with salinity) in 7 m water depth 4.5 km from the eastern shore of Bykovsky Peninsula. The thin dashed line indicates surface water temperatures of the Lena measured on the 10th, 20th and 30th of the month during the ice-free season over a 41-year period. The arrows indicate the axes of reference for conductivity (black arrow) and water temperature (grey arrow).

Instead, the 1975 image was referenced to WGS84 Universal Transverse Mercator 52 North projection using basic Russian topographic maps dating from the same approximate time and the rest of the images were co-registered to this 'base' image. A set of landforms considered stable over the observation period were determined on all seven sets of imagery to collect tie points. The number of tie points always exceeded 30 and corresponded to intersections of ice wedge polygon junctions, rare infrastructure or small stable ponds. Tie points were picked preferentially in low-lying areas to avoid relief distortion, as orthorectification of imagery was not possible due to the lack of information on the camera used for the aerial photographs and the impossibility of obtaining stereo-capable products for all the years studied.

The images were registered using off-the-shelf remote-sensing software. The root mean square (RMS) errors associated with the registration are listed in Table 1. RMS errors never exceeded 13 m and that particular high RMS error was associated only with the Resurs KFA-1000 image, which is understandable considering the low quality of this image. RMS errors for locations derived from the other images ranged up to 11 m. The coastline of the peninsula was manually digitized based on the 2006 SPOT-5 image. The presence of snow and heavy sediment loads in the coastal waters prompted the choice of manual digitizing over methods based on spectral information, which would have frequently misinterpreted the contour of the coastline. The digitized shoreline was then divided in 565 points seperated by an equal length. Erosion for the 1951–2006 period (or 1964–2006, where 1951 images were not available) was then calculated for each individual point. Sites for which estimation of erosion was too difficult were removed from the analysis. The resulting data set includes 494 sites. Erosion values computed from the movement of the cliff foot (or the shoreline, when the cliff foot was not clearly delineable) were converted to yearly rates of erosion.

The points were then selected to conduct analyses of the multi-period evolution of coastal erosion rates. Points characterized by erosion rates smaller than 1 m/yr were removed from the subsequent analysis since the retreat rates over four- to five-year periods at these sites were too small to be distinguishable from the RMS error induced by geospatial processing (i.e., maximum dilution of accuracy of 3.13 m for the 1964–69 period; see Table 2).

The 494 sites are distributed such that they face virtually all directions of wave attack. The subsampled sites, however, were much less representative and mostly located on coastline sections facing north-eastern, western and southern azimuths (Fig. 5).

Storm records

A database of storm events was constructed using the method specified by Atkinson (2005). The database was

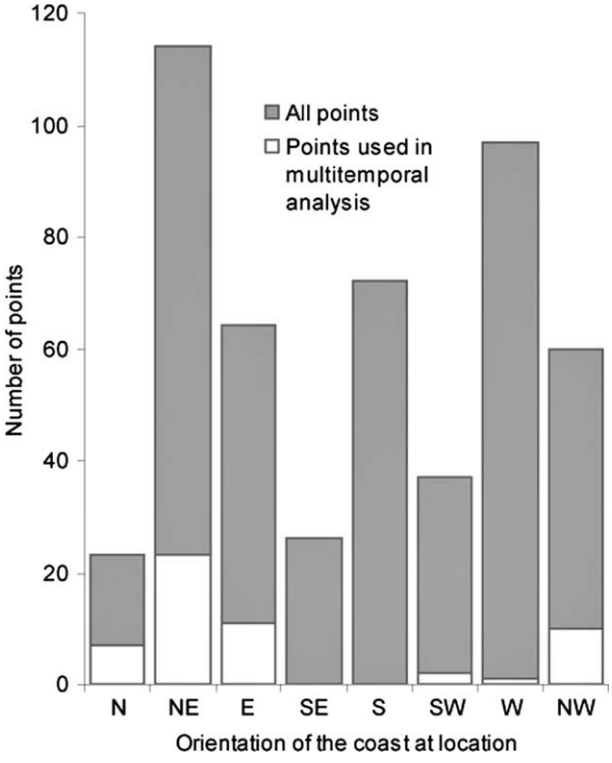

Fig. 5 Statistical distribution of shore orientation of the study sites. White areas refer to the number of sites used to compile rates for multiple periods. The number of multi-temporal sites is smaller because of the necessity of using sites characterized by large erosion rates to compute erosion rates over shorter periods of time.

Citation: *Polar Research* 2011, *30*, 7341, DOI: 10.3402/polar.v30i0.7341

derived using observational data gathered from two local weather stations: Tiksi (in operation from 1933 to the present) and Cape Bykovsky (in operation 1958–1989; see Fig. 2 for locations). The data sets exhibited variable observing regimes, including periods of hourly observation and other periods of six-hourly observation (that is, one observation taken every six hours). To create a uniform basis from which to build a storm event database both data series were subsampled to six-hourly observations following Atkinson (2005) and the storm extraction algorithm was run on the subsampled data sets.

The method identifies a 'storm' as a wind event that exceeds 10 m/s speed for at least six hours. Wind direction is not a constraining parameter; instead prevalent wind direction is an output parameter that can be used for subsequent analysis. The speed threshold was set following other Arctic coastal studies that identified this speed as one able to generate waves that can cause impact at the coast (Eid & Cardone 1992; Solomon et al. 1994; Hudak & Young 2002). For a detailed description of the method, see Atkinson (2005). The meteorological records started in 1958, which leaves seven years (1951–58) of our erosion record without corresponding storm data. We arbitrarily constrained the open-water season to the four months and a half of the Arctic summer and autumn (1 June to 15 October) and extracted storm events that possessed start dates falling within that ttime window.

Results

Coastal rerosion

In this study both sedimentation and erosion were evaluated. Sedimentation in the coastal zone was mostly linked to littoral drift-driven depositional landforms such as sand/gravel spits and lagoons. The size and shape of some of these lagoons changed dramatically over the 50-year study period, in some cases reflecting possible changes in drift patterns and in other cases, in drift supply. However, positive shoreline position changes (that is, aggradation) were encountered at only 25 study sites; apart from these sites little beach development was observed. The changes associated with these sedimentary features were highly transitory (i.e., sand spits, lagoons, beach berms) and since they represent a very small proportion of the total coastal change, they will not be discussed further.

Coastal erosion rates were first compiled for the 1951–2006 period and for the 1964–2006 period at sites where 1951 aerial photographs were not available (see Fig. 2). The mean yearly coastal retreat rate for all sites was 0.59 m/yr or around 30 m of shoreline retreat. This is comparable to, if not lower than, rates observed in other Arctic regions. Lantuit & Pollard (2008) found a rate of 0.61 m/yr on similar ice-rich coasts in northern Canada. Solomon (2005) indicated rates of 0.6 m/yr for the 1972–2000 period in the Beaufort–Mackenzie region, slightly lower than the ones found by Harper (1990) for the 1972–1985 period (1–2 m/yr). Mars & Houseknecht (2007) found greater rates, ranging from 1.4 m/yr to 5.4 m/yr, along a coastal section of the Alaska Coastal Plain but generally rates of erosion along the Alaskan Coastal Plain are lower (Jorgenson & Brown 2005). Total changes for the 1951–2006 period ranged from –434 m of erosion (8.35 m/yr) to 92 m of accretion (m/yr) and exhibited large variability ($\sigma = 45.4$). Sites with the largest changes (>100 m erosion) were clustered together in four small zones along the coastline; conversely, 97.0% of the rates observed were less than 2 m/yr and 81.6% were less than 1 m/yr (Fig. 6).

The largest erosion totals were observed on the north- and north-east-facing shores of the peninsula (1.05 and 0.97 m/yr, respectively) and the smallest on the south-east-facing shores (0.27 m/yr). All other sectors featured mean erosion rates ranging from 0.42 to 0.61 m/yr (Fig. 7). Erosion rates are mapped in Fig. 8. In addition to exhibiting the largest rates of erosion, the north- and north-east-facing shores also exhibited the largest standard deviations ($\sigma_N = 1.77$ and $\sigma_{NE} = 1.22$, respectively, while other sectors feature $\sigma < 0.6$). These sites also had all of the few extreme erosion values observed along the coastline. All sites featuring erosion rates greater than 2.5 m/yr are facing the north and the north-east. It is worth nothing that these extreme erosion sites are often located in settings prone to erosion such as capes or protruding sections of coasts, or in short sections of coasts characterized by changes in cryolithology. The orientation of the coast therefore seems to be at least of secondary order in explaining these strong values.

It is remarkable to observe that the east- and west-facing shores feature fairly similar mean erosion rates of erosion (0.57 m/yr vs. 0.56 m/yr), although most of the peninsula's western shoreline is facing an enclosed shallow bay (<2 m deep) bordered on its western side by the Kharaulakh Ridge with a evaluations up to 500 m a.s.l. The relatively constrained width of the bay combined with its shallow depth limits the height of waves that can potentially form on the western side of the peninsula and the presence of the ridge will limit wind speeds, which will further limit wave heights. Conversely, except for the north- and north-east-facing shores, the sections of coastline potentially exposed to waves

Table 3 Erosion rates and coastal types.

Coastal type	Rate (m/yr)	Standard deviation	Site count	Lower quartile (m/yr)	Higher quartile (m/yr)
Accretional sand bar	0.40	0.56	22	0.00	0.60
Alas	1.02	1.38	115	0.35	1.10
Ice Complex cliff	0.47	0.46	255	0.00	0.69
Lagoon barrier	0.47	0.35	41	0.16	0.80
Retrogressive thaw slumps	0.91	0.75	60	0.28	1.35
Total	0.65	0.84	493	0.16	0.86

formed in the offshore zone are not characterized by large erosion rates. There are other variables that explain the differences in the strength of erosion along the coastline.

Coastal evolution on the Bykovsky Peninsula is strongly influenced by the local lithology and geomorphology (Fig. 9). It is not unusual to observe neighbouring sites (hundreds of metres apart) along the coastline featuring very different erosion rates that can often be associated with changes in the nature of the backshore material. Sites located in alases (large depressions of the ground surface produced by thawing of very thick and exceedingly ice-rich permafrost [van Everdingen 1998]) are affected by strong erosion rates, while sites barred by cliffs undergo smaller erosion rates. The smallest retreat rates are always associated with sand bars, followed by lagoon barriers, coastal cliffs (Ice Complex), retrogressive thaw slump-affected coasts and alases (Table 3). The small rates associated with sand bars are a bias of the method used to calculate those rates and do not necessarily reflect an erosion of the backshore part of the coast but rather the rapid movement of longshore sedimentary forms following the release of sediment by thermal denudation and/or thermal abrasion. The run of several Student's t-tests to assess the significance of the difference between the mean erosion rates observed for the different coastal types indicates two groups of coastal types that are statistically different (at a 95% level of confidence), one comprising sand bars, lagoon barriers and coastal cliffs and the other comprising retrogressive thaw slump coasts and alases. Within each group the differences between the mean erosion rates observed for each coastal type are far from being significant. Between the two groups, however, the differences are always statistically significant at a 95% confidence level and even at a 99% level of confidence in four out of five tested differences. The large differences in coastal erosion rates are common along Arctic coasts (e.g., Solomon

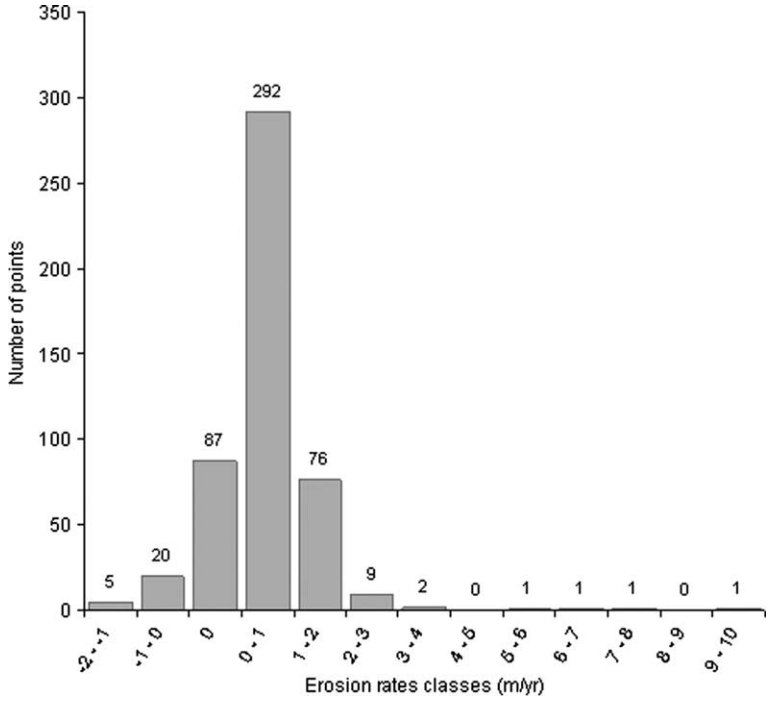

Fig. 6 Statistical distribution of erosion rates in classes of erosion strength (m/yr).

Citation: *Polar Research* 2011, *30*, 7341, DOI: 10.3402/polar.v30i0.7341

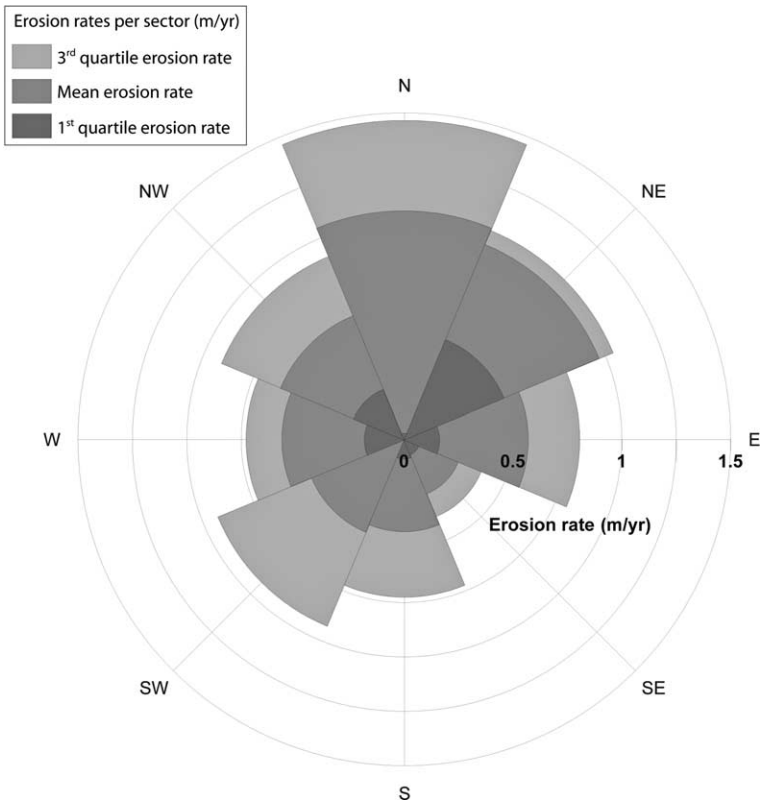

Fig. 7 Erosion rate strength (m/yr) and variability depending on shore orientation. The division by quartiles illustrate the large variability in the observed erosion rates.

2005) and can be explained by the geotechnical characteristics of the coast. Ice-rich cliffs such as the ones illustrated in Fig. 1 are eroded during storms through thermal abrasion. The erosion process requires great amounts of incoming wave energy to remove the beach sediments and the thawed overburden and to overcome the latent heat release associated with phase change and melt the cohesive ice matrix. The sediment cohesion is virtually null; the material strength is derived almost exclusively from the ice matrix. When these coasts are affected by thermal denudation processes, such as the ones featured in Fig. 10, part of the exposure is already thawed when the bottom of the cliff is affected by hydrodynamical processes, reducing the amount of thermal energy necessary to erode coastal material. A similar process has been observed by Lantuit & Pollard (2008) on Herschel Island, whereby intense retrogressive thaw slump activity had considerably lowered the shore profile, hence increasing the impact of erosion in a general context of decreasing rates. Alases (Fig. 11) are the end member of the thermokarst development: following the thaw of ice-rich sediments and often the formation of a thermokarst lake in a depression, the ground subsides, the lake expands but is eventually drained resulting in the apparition of an alas. Alas sediments are organic-rich, sediment-poor and are neither as high nor as ice-rich as either Ice Complex coasts or retrogressive thaw slumps-affected coasts. This facilitates the thermal abrasion process and results in higher rates on alas coasts. The highest rates of erosion were observed in an alas located in the south-east part of the island (Fig. 12) resulting in rates close to 10 m/yr in one location. However, these strong erosion rates are often associated with short stretches of coast. Rapid erosion on alas coasts also creates embayments that ultimately reduce the impact of hydrodynamic forcing, by diffracting waves on the lower gradient shorelines. The large range of retreat rates observed on alas coasts is primarily related to the geometry of the coastline.

A combination of geometry and cryolithology seems to explain a large part of the differences in erosion observed on the peninsula, but these combinations are so site-specific, in that only a few measurements have been taken for each combination, that it would prove challenging at this stage to extract patterns relevant to other sections of coast in the Arctic. Temporal records were obtained for six periods within the project time frame, 1951 to 2006. The data suggested no significant temporal

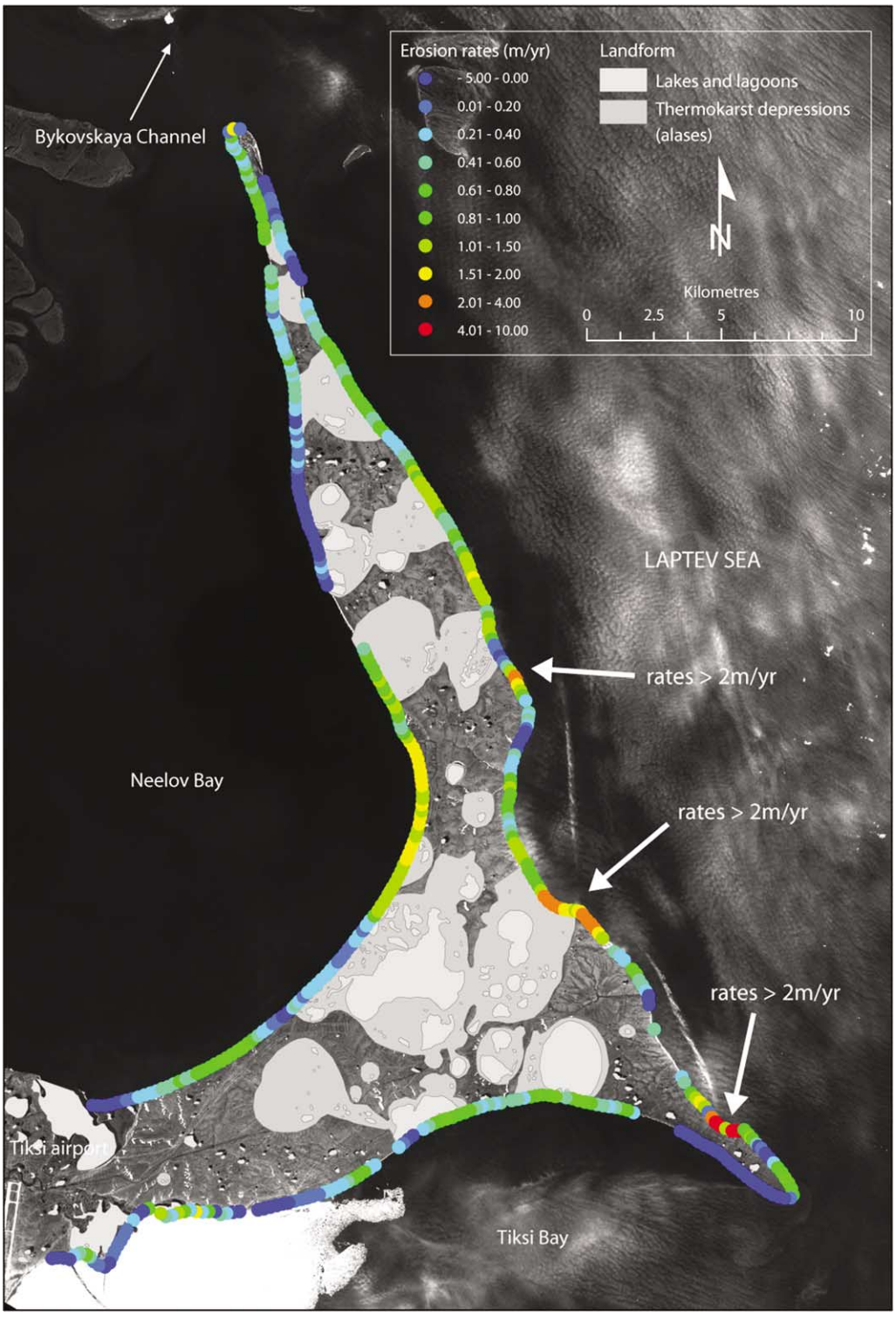

Fig. 8 Coastal erosion rates on the shores of the Bykovsky Peninsula.

Citation: *Polar Research* 2011, *30*, 7341, DOI: 10.3402/polar.v30i0.7341

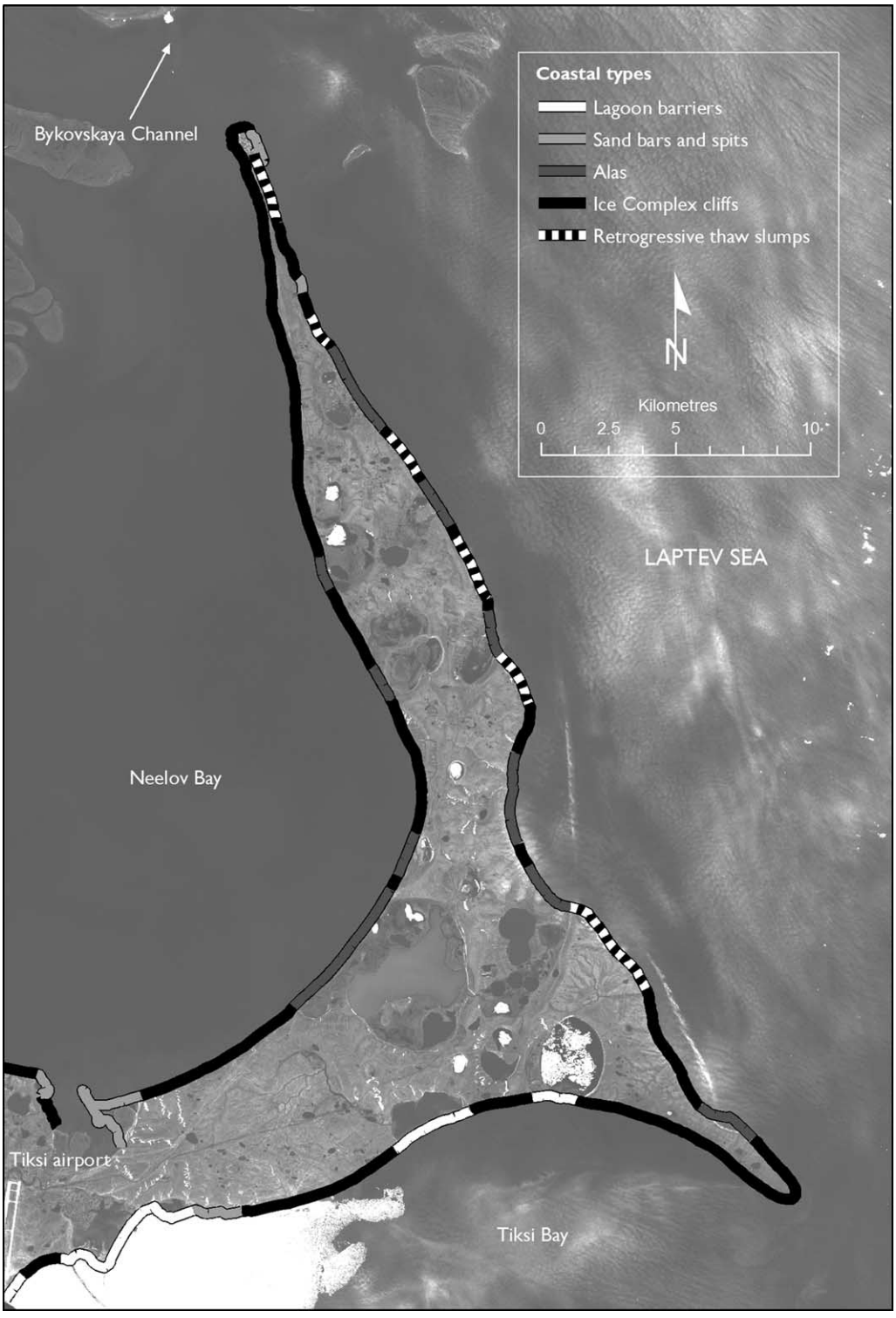

Fig. 9 Coastal types on the shores of the Bykovsky Peninsula.

Fig. 10 Retrogressive thaw slump on the coast of the Bykovsky Peninsula. The picture is taken from the edge of the slump. Note the presence of Baydzarakhs (earth mounds left in place after melting of coalesced ice wedges) within the slump floor. A man in the background gives the scale of the headscarp and is indicated by the black arrow.

trend in erosion (Fig. 13) but strong interannual to interdecadal variability. Mean erosion rates for the points subsampled for temporal analysis ranged from 1.09 m/yr (1986–2006) to 2.06 m/yr (1975–1981). On the Bykovsky Peninsula, rates of erosion can vary by one order of magnitude from one decade to the other, making it challenging to assert a reliable trend. Longer time series will be needed to subdue the interannual and interdecadal variability.

Meteorological records

Between 1958 and 2006 there were 665 storms recorded for Tiksi (Fig. 14); that is, around 13.6 storms a year

Fig. 11 Coastline in alas north of Mamontovy Khayata on the eastern shore of the Peninsula. The peat-rich alas low grounds are rapidly eroded by incident wave attack.

Citation: *Polar Research* 2011, *30*, 7341, DOI: 10.3402/polar.v30i0.7341

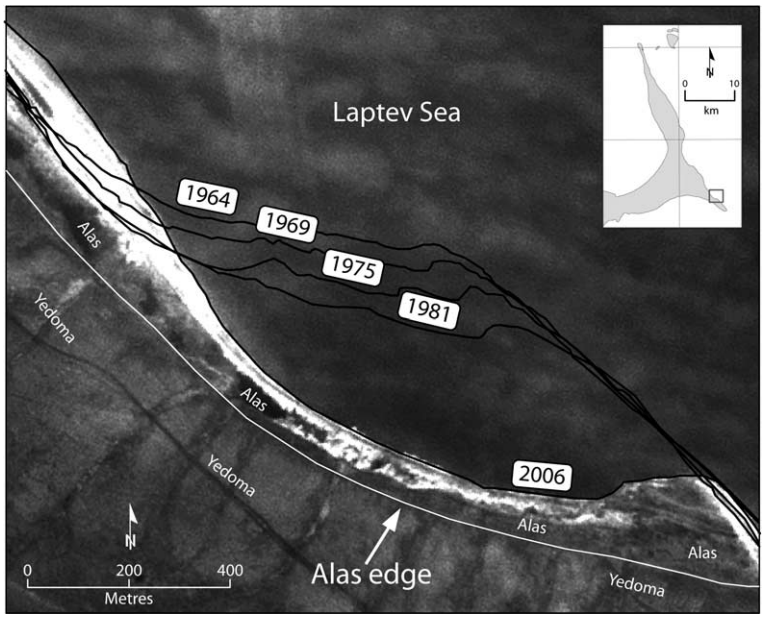

Fig. 12 Erosional sequence on an alas shoreline in the south-east part of the Peninsula. Alas is on the seaward side of the edge. The current shoreline is close to the edge of the alas, which should result in a significant decrease in coastal erosion rates on this stretch of coastline.

between 1 June and 15 October. The variance within the subsampled time interval was important ($\sigma = 7.9$) and reflects the strong interannual variability in storm counts. Six years featured no storms and three years featured more than 25 storms during the four months and a half summer interval (1969, 1970 and 1994). No significant trend in storm counts was observed at the Tiksi harbour, unlike other places in the Arctic according to some other studies (Serreze et al. 1993; Savelieva et al. 2000). Instead, periods of increased activity were noted. From 1958 to 1973, wind records are characterized by a strong variability, including several years with no storm activity and others with large storm counts. This period is followed by a period of relatively low but consistent activity (1973–1986), slightly less variable than the early period. After 1986, rates rise and remain high and steady until 1994. After 1994, the level of activity drops and a period of storminess decline is entered that persists up to 2001. The following five years (2002–06) feature a similar behaviour to the 1986–1994 period with storm counts steadily above average.

A summary of the mean direction of storm winds for the 1958–2006 period at the Tiksi weather stations are shown in Fig. 15. Of the 665 storms recorded during the investigation period, 69% exhibited dominant wind direction from the north-west, west and south-west, with 54% from the west and south-west. This distribution of storm primary wind direction is fairly consistent from decade to decade. We compared the before- and after-1986 periods (Table 4) and found similar distributions. Storms winds at Tiksi originate primarily and steadily from the west and south-west, moving over the

Table 4 Direction of storms for the 1958–1986 and 1987–2006 periods and for the 25% strongest storms that occurred over the 1958–2006 period.

Storm direction	1958–1986 Storm count (%)	1987–2006 Storm count (%)	Quartile strongest storms Storm count (%)
north	26 (6.8)	12 (4.3)	5 (3.0)
north-east	21 (5.5)	7 (2.5)	1 (0.6)
east	41 (10.7)	25 (8.9)	9 (5.4)
south-east	21 (5.5)	16 (5.7)	0 (0.0)
south-east	15 (3.9)	24 (8.5)	13 (7.8)
south-west	98 (25.6)	84 (29.8)	58 (34.9)
west	103 (26.9)	77 (27.3)	59 (35.5)
north-west	58 (15.1)	37 (13.1)	21 (12.7)
Total	383 (100)	282 (100)	166 (100)

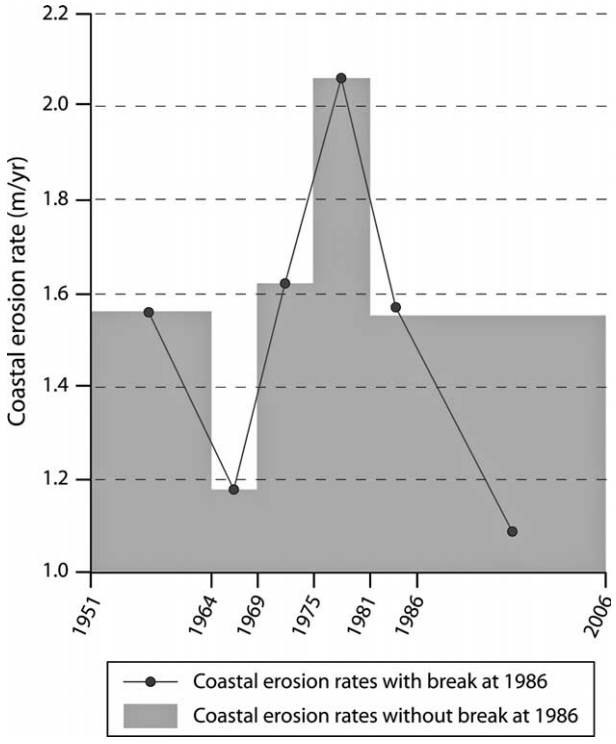

Fig. 13 Temporal evolution of coastal erosion. Two data sets are presented in this figure. One shows all periods investigated in this study (grey bars) and the other shows the same data without the 1986 date, which is based on a low resolution image (line).

bay but opposite the direction necessary to favour wave development from the open ocean. The 25% strongest storms recorded also showed a similar directional distribution clustering around the west, south-west and north-west (83% of the strongest storms originated from these azimuths).

Coastal erosion vs. storm counts

Direct relations between storm records and erosion observations are often hard to establish, when the impacts of individual storms cannot be resolved and when various confounding influences are present (e.g., variable sea ice, water levels, sediments/ground ice contents). A direct relation between storminess and erosion for the Bykovsky Peninsula is essentially nonexistent for the 1958–2006 period. Our erosion record is not detailed enough to conduct a formal statistical analysis of the relation between erosion and storminess at the Tiksi weather erosion; however, even the larger temporal peaks in erosion seem not to match peaks in storminess at the coast. A 'lag effect' (Solomon & Covill 1995; Lantuit & Pollard 2008) is often observed on ice-rich coasts and consists of the delayed movement of the shoreline following major storms due to the presence of large collapsed blocks in the coastal zone, which can take up to two or three years to be eroded. However, no lag effect could be identified on the Bykovsky Peninsula to explain the lack of coincidence between erosion records and storminess. Our record does not allow us to capture the height of storm surges along the coast and it is likely that one or two very large storms have a greater effect than the accumulated impacts of small storms, which could also explain some of the discrepancies between the meteorological and erosion records.

The spatial distribution of the main erosion zones and main storm directions are also strongly discordant. West-, north-west- and south-west-facing shores are not characterized by the strongest erosion rates, although storms winds in Tiksi favour these directions. The relatively small and shallow bodies of water located offshore in these directions explains these average rates of erosion. The fact that erosional features are nonetheless observed ubiquitously on the west-facing shores of the peninsula is actually evidence for the formation of high-power waves over very small water bodies. The wave height potential on the western shore is low (0.8 m) but it does compare with coasts possessing full ocean exposure (1.1 m).

Strong storm winds originating from the west are therefore probably needed to develop these waves but other factors such as warmer temperatures and large spring freshwater discharges from the Lena into Neelov Bay in delaying the fast ice formation (Eicken et al. 2005) and therefore lengthening the open-water season, despite the fact that Neelov Bay in delaying the fast ice formation (Eicken et al. 2005) and therefore lengthening the open-water season, despite the fact that Neelov Bay generally becomes ice-free after the waters to the east of the peninsula.

There are several likely reasons why the largest rates of erosion (north- and north-west-facing shores) are not associated with directions favourable to large wave development (e.g., not facing the predominant wind direction). First, as mentioned above, the relief constrains the formation of efficient storm surges and the angle of attack free of topographical obstacle to the Bykovsky Peninsula is limited to the spectrum where the strongest erosion rates have been recorded. Second, the number of study sites used to record erosion on north-facing shores is small and characterized by a great intravariability (see Fig. 4). Several of these sites are additionally located at Cape Bykovsky and are morphologically likely to endure stronger erosion rates due to the protruding shape of the cape. Third, the eastern coast is affected by strong thermokarst development and by the presence of a large alas in the south-west part of the peninsula, which has

Citation: *Polar Research* 2011, *30*, 7341, DOI: 10.3402/polar.v30i0.7341

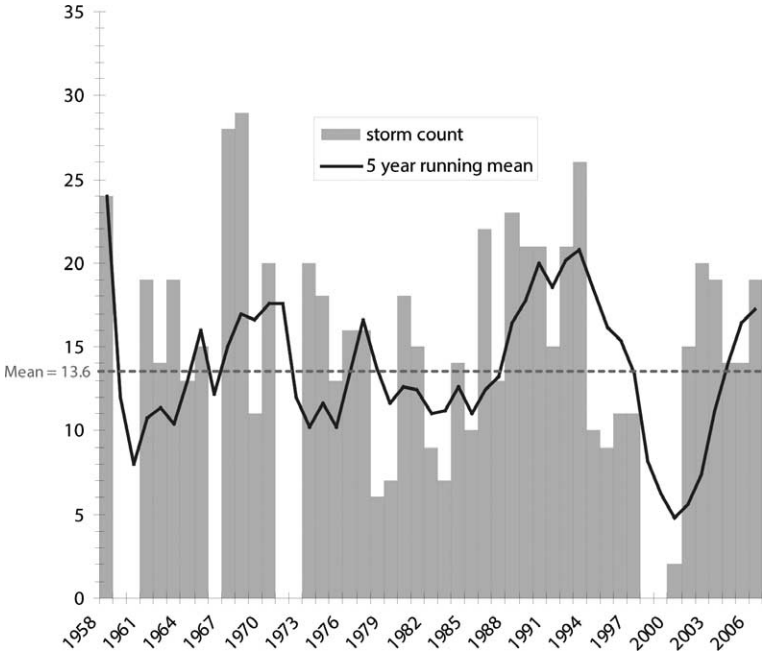

Fig. 14 Temporal evolution of storminess at the Tiksi station, 1958–2006. The histogram bars represent storm count.

been exhibiting the largest rates of erosion of the whole peninsula. In this case, the large erosion rates seem to be constrained by the morphological and cryological nature of the coast.

Discussion

Relating meteorological records to erosion data in our study and in others in the Arctic is difficult. Higher frequency of erosion measurements, as well as temporally detailed records of ice onset/offset, wave currents and water level, are needed to overcome these challenges. The storm data presented in this study are based on the Tiksi weather station, which is located on land and records the atmospheric pressure and wind data at the location of erosion (or very close to it). The wind data are used as a proxy for storminess and storm surges but this is a shortcut because wind data over offshore zones (where waves are formed) are not recorded in the area. A part of the apparent discrepancy in time between erosion data and storminess might actually be due to the flawed representation of storms in the nearshore zone when using local weather data instead of offshore wind fields.

Water level fluctuations of the Lena river and the presence of sea ice can probably also explain the discrepancy between erosion data and storminess. Water levels around the Bykovsky Peninsula are also controlled by the annual fluvial discharge regime of the Lena (and not necessarily by the limited tide action). High-water stands at the Bykovsky Peninsula occur while significant amounts of ice are present on the beaches and close to shore and while ground temperatures at the coast are very cold. Both factors tend to reduce the influence of spring high-water stands on erosion rates. More information is required, however, to distinguish the relative contributions of spring discharge and late summer storms to annual erosion rates. Another assumption used in this study is a fixed period for sea-ice offset/onset to compute the number of storms potentially impacting the coast during the open-water season. Because of the lack of any high-resolution near-shore sea-ice records for the study region this period was arbitrarily based on the mean open-water season length. In reality however, sea-ice onset and offset vary from year to year. The applied method might therefore result in slight under- or over-estimation of actual open-water season storm counts. Neither does the record allow us to resolve the wave set-up resulting from individual storms, which makes it difficult to evaluate the geomorphological impact of each storm.

Variations in temperature or salinity as described for the coastal section of the study area might be associated with differences in the timing of ice-on and ice-off events to the west and east of the peninsula. These are largely controlled by the spring freshet dislodging ice on the eastern side of the peninsula, while sea ice on the western side degrades in situ considerably longer before leaving Neelov Bay. Compared to less fluvially influenced

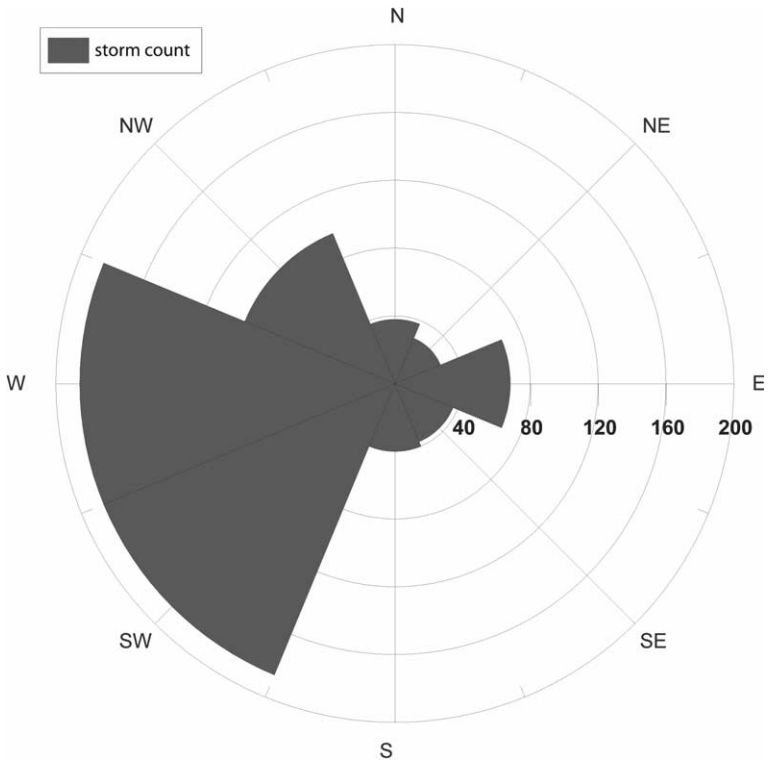

Fig. 15 Spatial distribution of storm wind directions recorded at the Tiksi station over the period 1958–2006. The radius represents storm count.

coastal sections thermo-erosional processes are probably more rapid in such a setting where fresher and warmer water is the main erosional agent. In the late season, however, waters in the Neelov Bay are probably warmer and frequent exposure to relatively small waves and mild surges driving very warm water into the cliffs could balance the less frequent, but potentially larger wave events on the east-facing side. We see little systematic difference in coastline retreat rates when comparing the eastern and western coastal sections. The spatial variability of coastal change rates is thus more likely the result of the interaction of meteorological forcing factors and water temperatures with the geomorphology of the shoreline.

A greater effort should be put into shoreline monitoring in several sites of the Arctic shoreline to resolve interannual variability in coastal erosion as well as better representation of storm surges through hindcasts of regional wind and pressure fields fields, and better data sets of coastal sea ice (both fast ice and pack ice), freshwater water levels and detailed bathymetry.

Decreasing sea-ice extent, longer open-water season and potential longer fetches should lead to stronger rates of erosion (Maxwell 1997; Anisimov et al. 2007) but little evidence is yet available to support this hypothesis in a consistent manner throughout the Arctic. Our records are consistent with observations by Aré (1988) who reported that "thermal erosion occurs very unevenly in time" on the Bykovsky Peninsula (Aré 1988: 117). Solomon (2005) and Lantuit & Pollard (2008) found stable to decreasing trends in coastal erosion on the southern Canadian Beaufort Sea coast. Mars & Houseknecht (2007), Jones et al. (2009) and Aguirre et al. (2008) found dramatically increasing rates of erosion for short stretches of coast on the North Slope of Alaska, but focused on low-lying, lake-rich silt and organic material, similar to that observed in alases on the Bykovsky Peninsula. Vasiliev (2003) and Vasiliev et al. (2005), using one of the only annual records of erosion on Arctic coasts, highlighted the strong interannual variability in coastal erosion rates and the possible connections to the Arctic Oscillation. Trends are hard to assess because of the lack of data to achieve statistical significance. This is primarily related to the strong interannual to interdecadal variability in both erosion and storminess. This again prompts the need for data sets with better temporal resolution and with longer time coverage. There are almost no places where coastal erosion has been recorded yearly in the Arctic. Former Soviet stations in the Barents, Kara and Laptev seas had records matching those standards until the late 1980s but the surveys were often discontinued before starting again

Citation: *Polar Research* 2011, *30*, 7341, DOI: 10.3402/polar.v30i0.7341

in the early 2000s. The current trends are currently being obliterated by the strong interannual variability in both erosion and storminess and several more decades of yearly erosion and storm records will be needed to improve the quality of our charts in the case of the Bykovsky Peninsula.

The absence of trend for the 1951–2006 period is, however, not an indication that erosion will remain steady over the next decades and/or centuries on the Bykovsky Peninsula. Atkinson (2005) showed that the greatest amount of storms, independently of the presence of sea ice, occurred in June and in October in the Laptev Sea area. Under changing sea-ice conditions and lengthening of the open-water season, the number of storms affecting the coasts (as recorded in Tiksi) could potentially double in a few decades. An ice-free Arctic ocean in the summer in 2040—or even in 2025 as reported by Holland et al. (2006)—would, however, not only lengthen the open-water season but also potentially modify the dynamics of storms in this region of the Arctic, with subsequent impacts on the magnitude of the surges and waves observed during storms. Until better characterization of the relation between storminess and erosion is available, the magnitude of the increase in coastal erosion will be difficult to assess but the recent drop in summer sea-ice extent (Stroeve et al. 2007) provides an incentive to re-visit shore protection measures in the Arctic region.

Conclusion

This paper builds on a long tradition of Russian scientific investigations in the Tiksi area to provide an updated version of coastal erosion rates on the Bykovsky Peninsula. The rates observed along the more than 150 km of coast investigated are unsurprisingly highly spatially variable and highlight the strong role of the cryostratigraphic nature of sediments in the erosional process. Of the various stretches of coast, alases are prone to the strongest erosion, followed by retrogressive thaw slump-affected coasts and finally by Ice Complex coasts, which is not unlike other stretches of coasts in the Canadian and Alaskan Arctic.

Erosion rates also vary with time and are surprisingly poorly linked to storminess at the Tiksi Station. We observe that offshore winds, bathymetry data sets and background water levels could more successfully be employed to model storm surges and waves, and hence erosion, along the Bykovsky Peninsula shoreline. In addition, we acknowledge the need to consider the combined impact of individual storms, water levels, cryolithology, shoreface and onshore geometry, thermokarst and water temperature in driving the strength of erosion. We hypothesize that the strong storm winds from the west, north-west and south-west are constrained topographically by the Kharaulakh Ridge and by shallow bays (Neelov and Tiksi bays) hampering the development of large wave set-up, but that local water conditions might help to foster relatively large rates of erosion on these same shorelines. Better wind, water level, water temperature, sea-ice and bathymetrical records should help us to model and assess the role of storm surges in the erosional process.

The lack of a significant trend in coastal erosion over the past 60 years does not mean that the current modifications of the Arctic cryosphere will not affect the rhythm of erosion. In addition to enhanced thermokarst in the shore zone, the extension of the open-water season to the whole months of June and October, which are the stormiest in the area, could strongly modify the impact of surges. Readjustments of the shoreface profile would take place at a different pace than the current one and changing conditions at the land–water interface can be expected.

Acknowledgements

The authors wish to thank the Tiksi Hydrobase for logistical support during several expeditions to the Laptev Sea. The SPOT images (copyright Centre National d'Etudes Spatiales) were acquired through SPOT Image distribution/Optimising Access to SPOT Infrastructure for Science programme, which is funded by the European Commission, Directorate-General for Research. The authors wish to thank Lutz Schirrmeister and Sebastian Wetterich for their invaluable help preparing this manuscript and during fieldwork. S. Ogorodov, J. Brown and an anonymous reviewer contributed reviews that greatly helped to improve the manuscript. We are very thankful for the time spent on these reviews. This paper is a contribution to the Arctic Coastal Dynamics project of the International Permafrost Association and of the International Arctic Science Committee.

References

Adams M. 1807. Some account of a journey to the frozen sea, and of the discovery of the remains of a mammoth. *Philosophical Magazine 29*, 141–143.

Aguirre A. Tweedie C. E., Brown J. & Gaylord A. 2008. Erosion of the Barrow Environmental Observatory coastline 2003-2007, northern Alaska. In D.L. Kane et al. (eds.): *Proceedings of the Ninth International Conference on Permafrost*. Pp. 7–12. Fairbanks: Institute of Northern Engineering, University of Alaska Fairbanks.

Anisimov O.A., Vaughan D.G., Callaghan T.V., Furgal C., Marchant H., Prowse T.D., Vilhjálmsson H. & Walsh J.E. 2007. Polar regions (Arctic and Antarctic). In M.L. Parry, et al. (ed.): *Climate change 2007: impacts, adaptation and vulnerability. Contribution of Working Group II to the fourth assessment report of the Intergovernmental Panel on Climate Change*. Pp. 653–685. Cambridge: Cambridge University Press.

Arctic Climatology Project. 2000. In F. Fetterer & V. Radionov (eds.): *Environmental working group Arctic meteorology and climate atlas*. Boulder: National Snow and Ice Data Center. CD-ROM.

Aré F.E. 1988. *Thermal abrasion of sea coast. Polar Geography and Geology 12*. Silver Spring, MD: V.H. Winston.

Atkinson D.E. 2005. Observed storminess patterns and trends in the circum-Arctic coastal regime. *Geo-Marine Letters 25*, 98–109.

Bauch H.A., Mueller-Lupp T., Taldenkova E., Spielhagen R.F., Kassens H., Grootes P.M., Thiede J., Heinemeier J. & Petryashov V.V. 2001. Chronology of the Holocene transgression at the north Siberian margin. *Global and Planetary Change 31*, 125–139.

Bruun P. 1962. Sea-level rise as a cause of shore erosion. *Journal of the Waterways and Harbors Division 88*, 117–130.

Dallimore S.R., Wolfe S.A. & Solomon S.M. 1996. Influence of ground ice and permafrost on coastal evolution, Richards Island, Beaufort Sea coast, N.W.T. *Canadian Journal of Earth Sciences 33*, 664–675.

Dolan R., Fenster M.S. & Holme S.J. 1991. Temporal analysis of shoreline recession and accretion. *Journal of Coastal Research 7*, 723–744.

Eicken H., Dmitrenko I., Tyshko K., Darovskikh A., Dierking W., Blahak U., Groves J. & Kassens H. 2005. Zonation of the Laptev Sea landfast ice cover and its importance in a frozen estuary. *Global and Planetary Change 48*, 55–83.

Eid B.M. & Cardone V.J. 1992. *Beaufort Sea extreme waves study. Environmental studies research funds report 114*. Calgary: Environmental Studies Research Funds.

Fetterer F. (ed.) 2008. The poles. In D.H. Levinson & J.H. Lawrimore (eds.): *State of the climate in 2007. Special Supplement Bulletin of the American Meterological Society 89*, S85–S105.

Forbes D.L. & Taylor R.B. 1994. Ice in the shore zone and the geomorphology of cold coasts. *Progress in Physical Geography 18*, 59–89.

Grigor'ev [Grigoriev] M.N., Imaev V.S., Imaeva L.P., Koz'min B.M., Kunickij V.V. & Mikulenko K.I. 1996. *Geologija, sejsmičnost' merzlotnye processy Zapadnoj Jakutii. (Geology, seismicity and cryogenic processes of the Arctic areas of western Yakutia.)* Yakutsk: Yakut Scientific Center, Siberian Branch, Russian Academy of Sciences.

Grosse G., Schirrmeister L., Kunitsky V.V. & Hubberten H.-W. 2005. The use of corona images in remote sensing of periglacial geomorphology: an illustration from the NE Siberian coast. *Permafrost and Periglacial Processes 16*, 163–172.

Grosse G., Schirrmeister L., Siegert C., Kunitsky V.V., Slagoda E.A., Andreev A.A. & Dereviagyn A.Y. 2007. Geological and geomorphological evolution of a sedimentary periglacial landscape in northeast Siberia during the Late Quaternary. *Geomorphology 86*, 25–51.

Harper J.R. 1990. Morphology of the Canadian Beaufort Sea coast. *Marine Geology 91*, 75–91.

Héquette A. & Barnes P.W. 1990. Coastal retreat and shoreface profile variations in the Canadian Beaufort Sea. *Marine Geology 91*, 113–132.

Hmiznikov P.K. 1937. O razmyve beregov v more Laptevyh. (Erosion of the shores of the Laptev Sea.) In: *Severnyj morskoj put'. (Northern Sea Route.)* Pp. 122–133. Leningrad: Izdatel'stvo GUSMP.

Holland M.M., Bitz C.M. & Tremblay B. 2006. Future abrupt reductions in the summer Arctic sea ice. *Geophysical Research Letters 33*, L23503, doi: 10.1029/2006GL028024.

Hudak D.R. & Young J.M.C. 2002. Storm climatology of the southern Beaufort Sea. *Atmosphere–Ocean 40*, 145–158.

Jones B.M., Arp C.D., Jorgenson M.T., Hinkel K.M., Schmutz J.A. & Flint P.L. 2009. Increase in the rate and uniformity of coastline erosion in Arctic Alaska. *Geophysical Research Letters 36*, L03503, doi: 10.1029/2008GL036205.

Jones B.M., Hinkel K.M., Arp C.D. & Eisner W.R. 2008. Modern erosion rates and loss of coastal features and sites, Beaufort Sea coastline, Alaska. *Arctic 61*, 361–372.

Jorgenson M.T. & Brown J. 2005. Classification of the Alaskan Beaufort Sea coast and estimation of carbon and sediment inputs from coastal erosion. *Geo-Marine Letters 25*, 69–80.

Kljuev E.V. 1970. Termičeskaja abrazija pribrežnoj polosy poljarnyh morej. (Thermal abrasion of the near shore zones of polar seas.) *Bulletin of the All-Union Geographic Society 102*, 129–135.

Kobayashi N., Vidrine J.C., Nairn R.B. & Solomon S. 1999. Erosion of frozen cliffs due to storm surge on Beaufort Sea Coast. *Journal of Coastal Research 15*, 332–344.

Lantuit H. & Pollard W.H. 2005. Temporal stereophotogrammetric analysis of retrogressive thaw slumps on Herschel Island, Yukon Territory. *Natural Hazards and Earth System Science 5*, 413–423.

Lantuit H. & Pollard W.H. 2008. Fifty years of coastal erosion and retrogressive thaw slump activity on Herschel Island, southern Beaufort Sea, Yukon Territory, Canada. *Geomorphology 95*, 84–102.

Mackay J.R. 1972. Offshore permafrost and ground ice, southern Beaufort Sea. *Canadian Journal of Earth Science 9*, 1550-1561.

Mars J. & Houseknecht D. 2007. Quantitative remote sensing study indicates doubling of coastal erosion rate in past 50 yr along a segment of the Arctic coast of Alaska. *Geology 35*, 583–586.

Matushenko N. 2000. What can we offer? Russia is optimistic about the future of the NSR. In C.L. Ragner (ed.): *The 21st century—turning point for the Northern Sea Route? Proceedings of the Northern Sea Route User Conference, 18–20 November 1999, Oslo, Norway.* Vol. 307. Pp. 51–53. Berlin: Springer.

Maxwell B. 1997. *Responding to global climate change in Canada's Arctic. Volume II of the Canada Country Study: climate impacts and adaptation*. Downsview, ON: Environment Canada.

Meyer M., Dereviagin A.Y., Siegert C. & Hubberten H.-W. 2002. Paleoclimate studies on Bykovsky Peninsula, north Siberia—hydrogen and oxygen isotopes in ground ice. *Polarforschung 70*, 37–51.

Pavlova E.Y. & Dorozhkina M.V. 2002. The Holocene alluvial delta relief complex and hydrological regime of the Lena River delta. *Polarforschung 70*, 89–100.

Peel M.C., Finlayson B.L. & McMahon T.A. 2007. Updated world map of the Köppen-Geiger climate classification. *Hydrology and Earth Systems Sciences Discussions 4*, 439–473.

Rachold V., Bolshiyanov D.Y., Grigoriev M.N., Hubberten H.-W., Junker R., Kunitsky V.V., Merker F., Overduin P.P. & Schneider W. 2007. Near-shore Arctic subsea permafrost in transition. *Eos, Transactions of the American Geophysical Union 88*, 149–156.

Rachold V., Eicken H., Gordeev V.V., Grigoriev M.N., Hubberten H.-W., Lisitzin A.P., Shevchenko V.P. & Schirrmeister L. 2003. Modern terrigenous organic carbon input to the Arctic Ocean. In R. Stein & R.W. Macdonald (eds.): *Organic carbon cycle in the Arctic Ocean: present and past*. Pp. 33–55. Berlin: Springer.

Rachold V., Grigoriev M.N., Aré F.E., Solomon S., Reimnitz E., Kassens H. & Antonow M. 2000. Coastal erosion vs. riverine sediment discharge in the Arctic shelf seas. *International Journal of Earth Sciences 89*, 450–460.

Romanovskii N.N. & H.W. Hubberten 2001. Results of permafrost modelling of the lowlands and shelf of the Laptev Sea region, Russia. *Permafrost and Periglacial Processes 12*, 191–202.

Romanovskii N.N., Hubberten H.-W., Gavrilov A.V., Tumskoy V.E., Tipenko G.S., Grigoriev M.N. & Siegert C. 2000. Thermokarst and land–ocean interactions, Laptev Sea region, Russia. *Permafrost and Periglacial Processes 11*, 137–152.

Savelieva N.I., Semiletov I.P., Vasilevskaya L.N. & Pugach S.P. 2000. A climate shift in seasonal values of meteorological and hydrological parameters for northeastern Asia. *Progress in Oceanography 47*, 279–297.

Schirrmeister L., Siegert C., Kuznetsova T., Kuzmina S., Andreev A.A., Kienast F., Meyer H. & Bobrov A.A. 2002. Paleoenvironmental and paleoclimatic records from permafrost deposits in the Arctic region of northern Siberia. *Quaternary International 89*, 97–118.

Semiletov I.P., Savelieva N.I., Weller G.E., Pipko I.I., Pugach S.P., Gukov A.Y. & Vasilevskaya C.N. 2000. The dispersion of Siberian river flows into coastal waters: meteorological, hydrological and hydrochemical aspects. In E.L. Lewis (ed.): *The freshwater budget of the Arctic Ocean*. Pp. 323–366. Dordrecht: Kluwer Academic Press.

Serreze M.C., Box J.E., Barr R.G. & Walsh J.E. 1993. Characteristics of Arctic synoptic activity, 1952–1989. *Meteorology and Atmospheric Physics 51*, 147–164.

Siegert C., Schirrmeister L. & Babiy O. 2002. The sedimentological, mineralogical and geochemical composition of late Pleistocene deposits from the ice complex on the Bykovsky Peninsula, northern Siberia. *Polarforschung 70*, 3–11.

Solomon S.M. 2005. Spatial and temporal variability of shoreline change in the Beaufort–Mackenzie region, northwest territories, Canada. *Geo-Marine Letters 25*, 127–137.

Solomon S.M. & Covill R. 1995. Impacts of the September 1993 storm on the coastline at four sites along the Canadian Beaufort Sea coast. In: *Proceedings of the 1995 Canadian Coastal Conference*. Vol. 2. Pp. 779–795. Ottawa: National Research Council of Canada.

Solomon S.M., Forbes D.L. & Kierstead B. 1994. *Coastal impacts of climate change: Beaufort Sea erosion study. Open File no. 2890*. Ottawa: Geological Survey of Canada.

Stroeve J., Holland M.M., Meier W., Scambos T. & Serreze M. 2007. Arctic sea ice decline: faster than forecast. *Geophysical Research Letters 34*, L09501, doi: 10.1029/2007GL029703.

Sukhovey V.F. 1986. *Seas of the world ocean*. Leningrad: Hydrometeorological Publications.

van Everdingen R. (ed.) 1998 (revised May 2005). *Multi-language glossary of permafrost and related ground-ice terms*. Boulder, CO: National Snow and Ice Data Center/World Data.

Vasiliev A. 2003. Permafrost controls of coastal dynamics at the Marre-Sale key site, western Yamal. In M. Philips et al. (eds.): *Permafrost: proceedings of the 8th International Conference on Permafrost, Zurich, Switzerland, 21–25 July 2003. Vol. 2*. Pp. 1173–1178. Rotterdam: A.A. Balkema Publishers.

Vasiliev A., Kanevskiy M., Cherkashov G. & Vanshtein B. 2005. Coastal dynamics at the Barents and Kara Sea key sites. *Geo-Marine Letters 25*, 110–120.

Wolfe S.A., Kotler E. & Dallimore S.R. 2001. *Surficial characteristics and the distribution of thaw landforms (1970 to 1999), Shingle Point to Kay Point, Yukon Territory. Open File no. 4115*. Ottawa: Geological Survey of Canada.

Yang D., Kane D., Zhang Z., Legates D. & Goodison B. 2005. Bias-corrections of long-term (1973-2004) daily precipitation data over the northern regions. *Geophysical Research Letters 32*, L19501, doi: 10.1029/2005GL024057.